Published in final edited form as:
Biomed Microdevices. 2010 December ; 12(6): 1027–1041. doi:10.1007/s10544-010-9457-7.

A low resistance microfluidic system for the creation of stable concentration gradients in a defined 3D microenvironment

Ovid C. Amadi,
Harvard-MIT Division of Health Sciences and Technology, Massachusetts Institute of Technology, Cambridge, MA, USA. Cardiovascular Division, Brigham and Women's Hospital and Harvard Medical School, Boston, MA, USA

Matthew L. Steinhauser,
Cardiovascular Division, Brigham and Women's Hospital and Harvard Medical School, Boston, MA, USA

Yuichi Nishi,
Department of Molecular and Cellular Biology, Harvard University, Cambridge, MA, USA

Seok Chung,
School of Mechanical Engineering, Korea University, Seoul, South Korea

Roger D. Kamm,
Department of Biological Engineering, Massachusetts Institute of Technology, Cambridge, MA, USA. Department of Mechanical Engineering, Massachusetts Institute of Technology, Cambridge, MA, USA

Andrew P. McMahon, and
Department of Molecular and Cellular Biology, Harvard University, Cambridge, MA, USA. Harvard Stem Cell Institute, Harvard University, Cambridge, MA, USA

Richard T. Lee
Cardiovascular Division, Brigham and Women's Hospital and Harvard Medical School, Boston, MA, USA. Harvard Stem Cell Institute, Harvard University, Cambridge, MA, USA

Richard T. Lee: rlee@partners.org

Abstract

The advent of microfluidic technology allows control and interrogation of cell behavior by defining the local microenvironment with an assortment of biochemical and biophysical stimuli. Many approaches have been developed to create gradients of soluble factors, but the complexity of such systems or their inability to create defined and controllable chemical gradients has limited their widespread implementation. Here we describe a new microfluidic device which employs a parallel arrangement of wells and channels to create stable, linear concentration gradients in a gel region between a source and a sink well. Pressure gradients between the source and sink wells are dissipated through low resistance channels in parallel with the gel channel, thus minimizing the convection of solute in this region. We demonstrate the ability of the new device to quantitate chemotactic responses in a variety of cell types, yielding a complete profile of the migratory response and representing the total number of migrating cells and the distance each cell has

Correspondence to: Richard T. Lee, rlee@partners.org.

Electronic supplementary material The online version of this article (doi:10.1007/s10544-010-9457-7) contains supplementary material, which is available to authorized users.

migrated. Additionally we show the effect of concentration gradients of the morphogen Sonic hedgehog on the specification of differentiating neural progenitors in a 3-dimensional matrix.

Keywords

Microfluidic; Concentration gradient; Migration; Chemotaxis; Morphogen gradient; Morphogenesis

1 Introduction

Many important biological processes such as gastrulation and organogenesis (Montero and Heisenberg 2004; Laird et al. 2008), inflammation (Friedl and Weigelin 2008), and cancer metastasis (O'Hayre et al. 2008) depend on the directed movement or transcriptional response of cells to biochemical and biophysical stimuli. *In vitro* systems designed to study these cellular behaviors rely on the replication of local microenvironments, including the presentation of relevant stimuli in an appropriate spatiotemporal pattern. The micro-environment may include specific cell populations, extracellular matrix components, and soluble or immobilized chemical signals. In contrast to experiments with cells grown in 2-dimensional monolayers, 3-dimensional cell culture systems allow for the construction of microenvironments characterized by preservation of native cell-cell and cell-matrix interactions (Abbott 2003). Like cellular migration (Sun et al. 2004; Even-Ram and Yamada 2005; Zaman et al. 2005; Gabriel and John 2006; Smalley et al. 2006; Zaman et al. 2006; Ghibaudo et al. 2009), a variety of cellular functions are markedly affected by 3D environments. This has prompted the development of 3D scaffolds such as hydrogels and self-assembling peptides in which cells can be seeded and cultured (Cukierman et al. 2001; Smalley et al. 2006; Lee et al. 2008; Zhang et al. 2008).

Chemotaxis is the directed translocation of a cell under the influence of a soluble chemical gradient. Several methods, with varying limitations and degrees of complexity, have been developed to study cell chemotaxis. The Boyden chamber assay establishes a chemical gradient across a thin porous membrane through which cells migrate in the direction of the concentration gradient (Boyden 1962). In the under-agarose assay, cells migrate between a coverslip and an agarose gel toward a well containing the chemical species of interest (Nelson et al. 1975). The Zigmond and Dunn chamber assays offer improved visual observation of cells migrating across a bridge between two wells, one containing the chemoattractant (Zigmond 1977; Zicha et al. 1991). Most assays lack quantifiable or stable concentration gradients and assay migration in 2D rather than 3D, prompting recent efforts to define stable gradients in three dimensional geometries (Keenan and Folch 2008).

Chemical concentration gradients may decay due to transfer of solute from the source region to the sink region. In order to establish a stable linear concentration gradient between a source and sink, the two regions must be continuously maintained at maximum and minimum concentrations, respectively. This is commonly achieved by continuous flow that replenishes the source solute concentration and eliminates the growing sink concentration. In the "Y-shaped" microfluidic device, two laminar streams are combined in a microfluidic channel, and the solute diffuses between streams, creating a gradient perpendicular to the combined flow path (Lin and Butcher 2006). These gradients are formed in a channel in which cells can migrate in a 2D but not 3D environment. In another implementation of flow-maintained gradients in microfluidic channels, a hydrogel is placed between a source and sink channel through which cells migrate up the concentration gradient established across a gel (Saadi et al. 2007; Vickerman et al. 2008; Chung et al. 2009; Mack et al. 2009; Sudo et al. 2009). The maintenance of stable linear concentration gradients by continuous flow,

however, is subject to a number of practical limitations. If flow characteristics in the source and sink channels are not identical, a pressure gradient will develop and the resultant fluid flow between the two channels can disrupt the concentration gradient. Fluid flow within the channel or gel induces shear stress on cells, which can independently alter the underlying biology of interest (Garanich et al. 2005). Fluid flow also depletes factors secreted by cells that might function as autocrine or paracrine signals. Finally, the durations of typical chemotaxis assays range from hours to days, periods over which replenishment by continuous flow requires substantial quantities of medium and chemoattractant. While non-continuous flow devices can facilitate stable gradients by creating source and sink wells with volumes much larger than that of the gel region (Abhyankar et al. 2008), such devices are still subject to interstitial flow induced by inadvertent fluctuations in the pressure difference between the two wells.

Here we describe a simple microfluidic approach to create and maintain concentration gradients in a microfluidic device without the use of continuous flow. Source and sink concentrations are maintained by creating corresponding wells whose volumes are large relative to the diffusive flux through the connecting hydrogel channel. Interstitial flow is eliminated by connecting the source and sink wells with additional channels and reservoirs that serve as a resistor-capacitor (RC) circuit. Accordingly, any pressure gradients between the source and sink are dissipated by flow through the low impedance RC network rather than through the hydrogel channel. Gradients can thus be maintained for several days and used to study the migration of a variety of cell types, as shown here with vascular smooth muscle cells and platelet derived growth factor (PDGF-BB), endothelial cells and vascular endothelial growth factor (VEGF), and Jurkat T-lymphocytes and the stromal-derived factor-1 (SDF-1).

Stable concentration gradients may also be useful to study the effect of graded morphogen concentrations on the spatial differentiation of developing tissues. Sonic hedgehog (Shh) is a secreted morphogen that is important in the specification of neural subdomains along the ventral-dorsal axis of the developing vertebrate neural tube (Dessaud et al. 2008; Briscoe 2009). Olig2 and Nkx2.2 are two transcription factors that are characteristic of two different neural tube domains, and their expression is stimulated by Shh in a concentration and time dependent manner (Dessaud et al. 2007). Here we demonstrate the Shh concentration and time dependence of Olig2 and Nkx2.2 expression in differentiating embryonic stem cells in a 3-dimensional environment by exposing embryoid bodies to Shh gradients in our new device.

2 Experimental

2.1 Design of RC device

The Resistor–Capacitor (RC) Device is composed of three regions, an experimental (source) region, a central cell (sink) region, and a control region as shown in Fig. 1(a) and (b). The source and sink wells are separated by a hydrogel-filled channel across which the desired chemoattractant gradient is developed. The source well is connected to the source-reservoir well by a low resistance channel, and the sink well is similarly connected to the sink-reservoir well. Finally, the source-reservoir well and the sink-reservoir well are connected to each other. Solute in the source channel may diffuse or be convected via two paths: either through the hydrogel channel or through the reservoir channels. The control region is a mirror image of the source region and serves as an internal control for each experiment. The control well is connected to the sink well by a gel region but there is not a chemical gradient between the sink and control wells as they are both filled with control/untreated solutions. Thus a control gel region for direct comparison accompanies each experimental gel region on the same chip.

2.2 Fabrication of RC device

The microfluidic devices were fabricated as described elsewhere (Vickerman et al. 2008). Briefly, the device design was drawn using the computer aided design (CAD) software SolidWorks and DWGeditor (Dassault Systèmes SolidWorks Corp, Concord, MA). The CAD files were sent to the Stanford Microfluidics Foundry (Palo Alto, CA) for master wafer fabrication. In this process, a transparency photomask was used to cure SU-8 photoresist on a silicon wafer and produce the positive relief of the microfluidic design. The completed wafer underwent silanization in order to facilitate the removal of the replica material. Replica molds were made from liquid polydimethylsiloxane, PDMS, (Sylgard® 184 Silicone Elastomer Kit, Dow Corning, Midland, MI) that was cured at 80°C for 2 h. The PDMS chips were removed from the wafer and the wells were formed by punching holes with appropriately sized biopsy punches and needles. The devices were autoclaved, plasma treated (Harrick Expanded Plasma Cleaner, Harrick Plasma, Harrick, CA) and bonded to glass cover slips. Finally, devices were coated with poly-D-lysine (poly-D-lysine hydrobromide, 1 mg/ml; Sigma–Aldrich, St. Louis, MO) to promote hydrogel attachment to the PDMS and glass surfaces.

2.3 Loading of collagen hydrogel

A prepolymer collagen solution was prepared on ice by combining 10X phosphate buffered saline, 0.5N sodium hydroxide, deionized water and Rat Tail Collagen Type I (BD Biosciences, Franklin Lakes, NJ) to produce a final collagen concentration of 2 mg/ml at pH 7. As shown in Fig. 1(a), each 1.5 mm long gel channel is connected to a small gel filling port. Approximately 4 μL of the collagen solution were injected into each gel region through the corresponding gel filling port. Each device was subsequently placed in a humidity chamber at 37°C for 30 min to allow for collagen gel polymerization. The humidity chambers were assembled from empty pipette tip boxes, containing sterile water. Finally, the devices were loaded with PBS or appropriate cells and culture medium.

2.4 Characterization of concentration gradients

RC devices were filled with PBS. The PBS solution was aspirated from the source well and source reservoir. In a subset of experiments, these ports were then filled with a 25 μg/ml FITC conjugated to a 10 kDa dextran solution. Fluorescent images of the gel region were acquired every 1 h for 24 h or every 2 h for a period of 12 h daily for 6 days. The data were analyzed using MATLAB (Mathworks, Natick, MA) software. The devices were covered with a glass cover slip to prevent evaporation during the time lapse period.

A device with a gel region whose width expands with distance from the source, Fig. 1(f) inset, was fabricated to form a non-linear concentration gradient. Similarly to the characterization of the linear device, the wells, reservoirs and channels were filled with PBS and then the source well and source reservoir were filled with a 25 μg/ml FITC conjugated 10 kDa dextran solution. Images were acquired every 2 h for a total of 12 h.

2.5 Maintenance of concentration gradients with pressure disturbances

To evaluate the dissipation of pressure gradients, pressure gradients were introduced into devices with and without the bypass channels and reservoirs connecting the source and sink wells. In the device without the bypass channels the source well was filled with a FITC-dextran solution and a gradient was allowed to develop for 6 h. At this time an additional 10 μl of the FITC-dextran solution was added to the source well, and images were acquired every 10 min for 1 h. In the device with the bypass channels the source and source reservoir wells were filled with the FITC-dextran and the 10 μl bolus of the FITC-dextran solution was added to the source well.

In a separate experiment the source and source reservoir wells were filled with a 50 μg/ml FITC-dextran (20 kDa) and a 10 μl bolus of the FITC-dextran solution was added to the source well. Fluorescent images were taken of each well in the device before and 5 min after the introduction of the bolus. This images were used to calculate the average concentration in each well before and after the introduction of the bolus.

2.6 Cell migration assays

Vascular smooth muscle cells (VSMC's) were cultured in Dulbecco's Modified Eagle Medium (DMEM) supplemented with 1% penicillin/streptomycin, 1% L-glutamine and 10% fetal bovine serum (FBS). Bovine aortic endothelial cells (BAEC's) were cultured in DMEM supplemented with 1% penicillin/streptomycin and 10% FBS. Jurkat T lymphocytes cells were cultured in suspension with RPMI-1640 medium supplemented with 1% penicillin/streptomycin and 10% FBS. Immediately after the collagen gel polymerization, devices were filled with PBS to prevent any air bubble formation around the gel region. The PBS was aspirated from the device and the sink well was filled with 40 μL of a cell suspension at a concentration of 1×10^6 cells/ml. Ten μL of media were placed in the source and control wells to create a pressure gradient and thus interstitial flow from the sink well into the source well. This flow caused the cells to accumulate on the surface of the collagen gel. The devices were incubated for 3 h at 37° C in order to allow the cells to adhere to the collagen surface. The medium within the source and source reservoir wells was replaced with medium supplemented with PDGF-BB (4 nM), VEGF (0.1 nM and 1.0 nM), or SDF-1 (1.0 nM and 10 nM). The sink and sink reservoir wells were filled with un-supplemented control medium. To prevent evaporation without limiting gas exchange with the environment, devices were incubated in a high humidity chamber at 37°C and media was changed daily. After 48 h the devices were fixed with 4% paraformaldehyde and stained with DAPI. Fixing and staining were performed overnight to allow the PFA and DAPI molecules to diffuse throughout the gel region. Images of both the experimental and control gel regions were acquired at 10X magnification.

2.7 Data analysis

The location of each cell in each gel region was stored and categorized into bins at 100 μm increments into the gel. With sufficient magnification individual cells could be identified manually. When cells were closely crowded and difficult to distinguish from one another the manual identification tended to underestimate the number of cells, biasing the result toward the null hypothesis. In the VSMC (N=4) migration assay the bin data for the experimental and control regions were averaged and compared using a Student T-test. In the BAEC (N=5) and Jurkat (N=4) assays, the control bin data were first subtracted from the experimental bin data from each device. The scaled data were averaged for each concentration and compared using Student's T-test. Data were further analyzed using the Bonferroni correction for multiple comparisons.

2.8 Embryonic stem cell culture and differentiation

The Olig2-GFP reporter ES cell line was developed as described previously (Hai-Qing et al. 2003). An Nkx2.2-tdTomato reporter line was created by electroporating the construct in cells with a Rosa26-Gli1-FLAG background (Vokes et al. 2007). Cells were cultured separately on 0.1% gelatin coated flasks in Gasglow Minimum Essential Media supplemented with 15% KnockOut™ Serum, 1X Non-essential amino acids, 1X sodium pyruvate, 0.1 mM 2-mercaptoethanol, 1% penicillin-streptomycin, and 1,000 units/ml leukemia inhibitory factor (LIF).

To induce differentiation the Olig2-GFP and Nkx2.2-tdTomato cell lines were mixed in a 1:1 ratio in DFNB medium: DMEM-High glucose, F-12 Medium, and Neuro-basal Medium

in a 1:1:2 ratio supplemented with 1% penicillin-streptomycin, 1% L-glutamine, 10% KnockOut™ Serum, and 55 μM 2-mercaptoethanol. Hanging drops were formed with 500 cells per 12 μl droplet and embyroid bodies were allowed to form for 2 days.

2.9 Sonic hedgehog morphogen gradients

A collagen prepolymer solution was used to seed embryoid bodies in the RC devices. The solution was prepared on ice by combining 10X DMEM, deionized water and Rat Tail Collagen Type I to produce a final collagen concentration of 2 mg/ml at pH 7. Day 2 embryoid bodies were collected in a pellet, and approximately 6,500 embryoid bodies were added to 35 μl of the collagen pre-polymer solution. Approximately 4 μl of the suspension was injected into each gel region of the devices and the collagen was allowed to polymerize at 37°C for 30 min. Devices were then filled with DFNB medium supplemented with retinoic acid at a concentration of 500 mM. The source and source reservoir wells of each device were loaded with retinoic acid supplemented DFNB and recombinant Sonic Hedgehog protein (R&D Systems, Minneapolis, MN) at concentrations of 12.5 nM, 25 nM, 50 nM, and 125 nM. Media in the devices were changed every 24 h and images of the gel regions were acquired daily. The cells remained in the devices for 4 days.

3 Results and discussion

3.1 RC device dynamics

In evaluating and predicting gradient formation in the RC microfluidic device, the two relevant processes affecting the concentration profile are molecular diffusion and convection. Thus the governing mass transport equation is shown below:

$$\frac{\partial M}{\partial t} = -D\nabla^2 M + \vec{v}\cdot\nabla M$$

where M is the concentration, t is time, D is the diffusivity of the solute, and v is the velocity field. The first term accounts for the solute flux due to diffusion down a concentration gradient while the second term is generated by convection of the solute in a velocity field. The velocity field can be determined as a solution to the incompressible Navier-Stokes equation for the open channels. In the RC Device, the viscous stresses are of much greater magnitude than the inertial forces, allowing the inertial forces to be neglected in the analysis. Within the gel regions, the resistance due to the porous collagen scaffold must be included. The result is the Brinkman equation that models viscous flow through a porous material:

$$\mu\nabla^2\vec{v} - \frac{\mu}{K}\vec{v} - \nabla P = 0$$

where μ is the dynamic viscosity of the media, K is the permeability of the hydrogel, and P is the pressure. Coupling these two equations, one can model the complete behavior of the fluid flow and mass transport in the RC Device. The necessity of the low impedance reservoir channels is illustrated with the finite element model in Fig. 2(a). Here the device consists of only the source well, the sink well, and the interconnecting gel region. The source well is loaded with 1 mm of hydrostatic pressure (10 Pa), the result of adding 7.06 μl more fluid to the source well than the sink well. The simulation was performed for 1 h with SDF-1 as the soluble molecule. Initially the concentration in the source well was 100% and the concentration in the gel region and sink well was 0%. The velocity was everywhere zero. The diffusivity of SDF-1 is 1.6×10^{-6} cm^2/s in PBS (Veldkamp et al. 2008) which can be

assumed to approximate its diffusivity in a 0.2% w/v collagen gel. The permeability, *K*, of the collagen gel was taken to be 1×10^{-12} m^2 (Wang and Tarbell 2000). After 1 h the high concentration solution has been convected through the gel as a result of the increased source pressure. Under these conditions, the average velocity in the gel is 6.5 μm/s and the corresponding Peclet number (the ratio of convective to diffusive transport) is approximately 61, demonstrating the dominance of convection.

In order to prevent this convection, the low impedance reservoirs and channels were included to complete the design of the RC Device. Pressure differences between the source and sink wells are dissipated through the reservoir channels much more rapidly than through the gel region. The reservoirs decrease the change in concentration due to the exchange of fluid between the source and the sink. For instance, if there is more fluid in the source well than in the sink well, the fluid first flows to the source reservoir well, followed by the sink reservoir well, where this small volume needed to eliminate the pressure difference is diluted, before proceeding to the sink well itself. In an analogy to electrical circuits where volumetric flow rate is to electrical current as pressure gradients are to voltage drops, the RC device can be modeled as an arrangement of resistors and capacitors as shown in Fig. 1(c). Each of the channels in the device impose resistance on fluid flow and determine the flow rate for a given pressure difference. The volumetric flow rate, Q, of a viscous fluid through a channel with a rectangular cross-section is similar to the Hagen-Poiseuille equation for laminar, viscous and incompressible flow:

$$Q=\frac{W_c H_c^3}{12\mu L_c}\Delta P,$$

where W_c, H_c, and L_c are the width, height and length of the channel, respectively and ΔP is the pressure drop along the length of channel. The resistance of the channel, R_c, is the ratio of ΔP to *Q* (analogous to electrical resistance as the ratio of voltage to current through a resistor) and is given by the expression.

$$R_c=\frac{12\mu L_c}{W_c H_c^3}$$

In the gel region, the resistance to flow is dominated by the low permeability of the hydrogel. Darcy's Law governs the relationship between pressure and flow rate, their ratio yielding the resistance of the gel region, R_g.

$$Q=\frac{KW_g H_g}{\mu L_g}\Delta P \Rightarrow R_g=\frac{\mu L_g}{KW_g H_g}$$

The wells in the device store fluid volume just as a capacitor stores charge. The capacitance of a capacitor is the ratio of the charge stored in the capacitor and the voltage drop across it. In the wells the relationship between the pressure difference between the top and bottom of the well and the volume of fluid in the well is governed by hydrostatics, $\Delta P=\rho g h$, where ρ is the density of the fluid, *g* is the acceleration due to gravity, and *h* is the depth of the fluid. The depth of fluid in the well is determined by the volume of fluid in the well divided by the cross sectional area of the well. The capacitance of a well can then be defined as the ratio of volume to pressure difference,

$$\Delta P = \frac{4\rho g}{\pi D_w^2} V \Rightarrow C_w = \frac{\pi D_w^2}{4\rho g},$$

where V is the fluid volume in the well, D_w is the diameter of the well, and C_w is the capacitance of the well.

Using the values for the various dimensions in Fig. 1, the resistance of each reservoir channel is 6.94×10^{10} kg/m^{4}s, whereas the resistance of the gel filled channel is 2.80×10^{13} kg/m^{4}s, more than three orders of magnitude larger than it would be if the gel were not present. The capacitance of the source and sink wells is 7.21×10^{-10} m^{4}s^2/kg and the capacitance of the source and sink reservoirs is 1.28×10^{-9} m^{4}s^2/kg. In Fig. 1(c) one of the capacitors contains excess charge/voltage and must dissipate charge to the remaining three. There are two paths through which the current may travel, one containing the three channel resistors and the other containing the gel resistor. This process is analogous to the source well containing excess volume/pressure and dissipating this volume to the other sinks and reservoirs (neglecting the control side of the device). The channel path contains three resistors in series and four capacitors in parallel while the gel path contains one resistor and two capacitors in parallel. The solution to the characteristic equation for the voltage in each capacitor gives the time constant for the system (see Supplemental information). The time constant, τ_c, for flow through the channel path is on the order of 50 s, and the time constant, τ_g, for flow through the gel path is 168 min. Thus pressure gradients are quickly equilibrated through the channel path, preventing significant source solute convection into the gel.

To confirm the time constant we measured the velocity of suspended cells in the channel between the source and source reservoir well after a 7 μl bolus was added to the source well with a microneedle injector. The measured maximum velocity was 2.03±0.2 mm/s equal to a volumetric flow rate of 0.484 μl/s. At this flow rate the time required for the volume to be distributed throughout the device is approximately 15 s. This confirms that dissipation of pressure gradients occurs rapidly through the bypass channels but exhibits a more rapid time constant than had been calculated. The discrepancy is likely due to the momentum of the bolus as it was injected into the well which caused the fluid in the channels to accelerate more rapidly than if the driving force was a hydrostatic pressure difference alone.

3.2 Maintenance of stable concentration gradients

The generation and maintenance of a stable concentration gradient between the source and sink wells is determined by the diffusion coefficient of the biomolecule of interest and the geometry of the device. In Fig. 1(d), a 25 μg/ml solution of a 10 kDa FITC-Dextran in PBS was loaded into the source side of the RC device while the sink and control regions were filled with PBS. After 2 h a linear concentration gradient was present between the maximum concentration at the source well and the minimum concentration at the sink well. The gradient remained constant for the duration of the 24-hour experiment.

The duration of time over which the gradient will remain constant is a function of the dimensions of the source and sink wells and the hydrogel channel as well as the definition of “constant.” As the solute diffuses from the source well into the sink well, the concentration gradient will diminish and eventually vanish entirely. The flux of solute is the product of the diffusion coefficient and the gradient of the concentration field. If, for instance, a “constant” gradient is defined as a gradient in which the source and sink concentrations do not change by more than 5% (a 10% change in the gradient slope), then the gradient formed by an 8 kDa molecule would remain “constant” for more than 2 days. Similarly, the system would require approximately 21 days for concentrations in the source and sink wells to equilibrate

completely. These estimates presume that the wells are perfectly mixed but are confirmed by our experimental results. In Fig. 1(e) the slope of the concentration gradient was measured daily for a period of 6 days. During days 1 and 2 the gradient remains relatively stable. On day 3 the gradient had decayed by ~10% and by day 5 it has decayed further to 80% of the original value. The relative stability of the gradient over several days allows the schedule of medium changes in the device to be dictated by the metabolic requirements of the cells.

By changing the shape of the gel region it was possible to change the profile of the concentration gradient. In a device with an expanding gel region, Fig. 1(f), the concentration gradient adopts a nonlinear profile, exhibiting an exponential decay with distance from the source region. The gradient is developed in less than 2 h and remained constant for the duration of the 12 h experiment. The stability of the nonlinear gradient should be similar to that of the linear gradient. This is because the channels and wells (except for the gel region) are identical to those in the linear gradient device and the average flux through the gel region, determined by the source and sink concentration, is similar to the flux in the gel region with the linear gradient.

3.3 Sensitivity to pressure disruptions

A major advantage of the RC Device is its ability to dissipate pressure gradients through the low resistance reservoir channels as opposed to transporting fluid through the hydrogel region. Pressure gradients between the different wells or channels in a microfluidic device are often an inevitable consequence of handling the device during its operation. Fluid volumes must be precisely dispensed in and out of the device to prevent volumetric imbalances and hydrostatic pressure differences. These hydrostatic pressure differences result in fluid flow between adjacent wells. If this fluid flow occurs in the gel channel the concentration gradient will be disrupted. Pressure differences can also be caused by inadvertent tilting of the device which places one well at a higher gravitational potential relative to other wells.

While the stable concentration gradient is not affected by incidental pressure gradients created during the initial loading of the device (Fig. 1(d)), we also explored the effect of more substantial pressure gradients on the soluble profile in the hydrogel. We first characterized this process in a device without the bypass channels connecting the source and sink wells. This device contained only a source well and a control well each connected to the sink well through a gel region. The device was loaded with a 25 μg/ml solution of 10 kDa FITC-Dextran in the source well, and a linear gradient was allowed to develop for 6 h. At that time (t=0), an additional 10 μl bolus of dextran solution was added to the source well creating a hydrostatic pressure difference between the source and sink wells, Fig. 2(b). The concentration profile in the gel region was immediately disrupted as the FITC-dextran solution was convected through the gel in order to eliminate the pressure gradient. The concentration gradient was almost completely abolished as the concentration became relatively constant throughout the gel. After 6 h the concentration gradient had not returned to a linear profile confirming that the time scale for the system to reach equilibrium is on the order of hours as estimated above.

We repeated this experiment in the RC device with the channels and reservoir wells connecting the source and sink wells. Both the source well and source reservoir well were filled with the FITC-dextran solution. After the linear gradient had developed a 10 μl bolus of dextran solution was added to the source well. The concentration profile in the device did change immediately, as noted by comparing the initial and t=0 curves in Fig. 2(c). However only a small fraction of the additional solute was convected through the gel region, while the majority of the bolus was transported through the reservoir channels. As a result, within 10

min of the bolus introduction, the concentration gradient within the hydrogel has returned to a stable, linear profile.

To investigate how the flow through the bypass channels affects the concentration in the different wells we measured the concentration in each well before and after a 10 μl bolus was injected into the source well and the pressure gradients were eliminated, Fig. 2(d). The largest concentration change occurred in the sink reservoir well which receives high concentration fluid directly from the source reservoir well. The sink well did not experience a significant concentration change because any high concentration fluid that reaches the sink well is first diluted in the sink reservoir well. This dilution also occurs with the control reservoir and control wells, and their concentrations do not change after the introduction of the bolus.

3.4 VSMC migration toward PDGF-BB

Platelet derived growth factor has been shown to induce chemotaxis of vascular smooth muscle cells *in vitro* (Bornfeldt et al. 1994). Figure 3(a) shows the comparison of migration of VSMC's toward a 4.0 nM solution of PDGF-BB versus a control. The images have been reoriented such that in both the PDGF-BB and control cases, the direction of migration toward the PDGF-BB (or control) well is from left to right.

While is it clear that the response to PDGF-BB is greater than that of the control, it is difficult to comment definitively on the relative number of migrating cells and the distance these cells have migrated solely from the images. A single metric could be calculated to describe the chemotactic response but some information regarding the complete cell distribution would likely be lost. Figure 3(a) uses a histogram approach to compare the number of VSMC's which have migrated a given distance into the gel regions. At each distance, there were more cells present in the PDGF-BB gel region than at the corresponding distance in the control gel, achieving statistical significance in the 0–100 and the 100–200 μm ranges before the Bonferroni correction. In both cases the number of migrating cells decreased as one moves farther into the gel.

3.5 Jurkat T lymphocyte and endothelial cell chemotaxis

In addition to comparing migration toward a chemoattractant versus a control, we used RC Device to quantify a dose response for a single factor. Figure 3(b) and (c) compare the migration of Jurkat T Lymphocytes toward a known chemo-attractant SDF-1 (Hesselgesser et al. 1998) at two different concentrations, 1 nM and 10 nM, as well as the migration of bovine aortic endothelial cells to VEGF-A (Vernon and Sage 1999) at concentrations of 0.1 nM and 1 nM. Both cell types exhibited a dose-dependent chemotactic response, but cell-type differences in migratory patterns are observed. The Jurkat cells exhibited a similar response to the VSMC's in that the number of cells at each location decreases with increasing distance into the gel. In contrast, the maximal endothelial response occurs at an intermediate value, 400–600 μm. Both the high and low VEGF-A concentrations induced endothelial cells to migrate a short distance into the gel—the major difference between the responses occurring at an intermediate distance in the gel where there were markedly more cells in the high concentration case. The endothelial cells migrated as single cells and did not form tube-like structures as they entered the gel. This behavior is likely a result of the short time period in which the cells were allowed to form cell to cell contacts and organize into a monolayer before the chemotaxis assay began.

Media in the devices were replenished daily, but this process does not have a profound effect on the gradient and cell behavior for at least two reasons. First, we expect that during the brief time during which the source or sink well is empty the pressure difference will

cause flow primarily through the bypass channels as was the case after the 10 μl bolus injection. Second, as shown in Fig. 1(d), even if the gradient is disrupted during the media loading process the profile will return to a steady state value in less than 2 h.

3.6 Sonic hedgehog induced Olig2 and Nkx2.2 expression

Embryonic stem cells seeded in the collagen gel regions continued to proliferate, eventually merging into one large continuous mass covering the entire gel volume, Fig. 4(a). On day 0 a Shh gradient was formed in the gel regions containing the differentiating cells. Shh stimulates the expression of the transcription factors Olig2 and Nkx2.2 (Dessaud et al. 2007), and initially there was no Olig2 or Nkx2.2 expression detectable by fluorescent microscopy. On day 3, both Olig2 and Nkx2.2 expression became evident at the edge of the gel closest to the Shh source and by day 4 the expression had spread farther into the gel. The cells farther from the Shh source were exposed to lower Shh concentrations and required more Shh exposure time before activating expression of Olig2 and Nkx2.2, illustrating the interplay between Shh dosing concentration and dosing time in neural tube development. We compared these expression levels to those found in control gel regions that contained embryoid bodies that were not exposed to a Shh gradient. There, as shown in Fig. 4(b) and (c), the expression levels in the untreated gels were uniform at baseline levels. In the gels with the Shh gradient both Olig2 and Nkx2.2 expression levels were highest closest to the Shh source and decayed to the baseline untreated level approximately halfway between the Shh source and sink. This is consistent with the notion that in the portion of the gel where the Shh concentration exceeded some critical threshold, expression of Olig2 and Nkx2.2 was stimulated; in the remainder of the gel, where the Shh concentration was below the threshold, no such stimulation occurred.

We then examined the expression pattern created by different levels of Shh gradients, Fig. 5. As the concentration of the Shh source increased, the concentration at each point in the gel increased as well. Accordingly with increasing Shh source concentration the extent of Olig2 and Nkx2.2 expression into the gel region increased. As distance from the Shh source increased, the fluorescent signal eventually faded to the baseline level present in the control gels. The point at which the fluorescent intensity reached the untreated baseline level is plotted as a function of the Shh source concentration in Fig. 5(c). This point, measured as distance from the Shh source well, is the location of the threshold concentration, which moves farther into the gel with increasing source concentration. The threshold locations were similar for the Olig2 and Nkx2.2 reporter lines, indicating a common threshold for the expression of the two transcription factors. This result is likely due to the constitutive Gli1 expression (Vokes et al. 2007) or the absence of additional signaling factors that also modulate neural tube patterning (Joong Yull et al. 2009; Ulloa and Martì 2010) and the relatively long half-life of GFP and tdTomato. Analysis of the position of the threshold in the linear Shh gradient indicates that the threshold concentration for Olig2 and Nkx2.2 was approximately 10 nM Shh.

4 Conclusion

Here we have presented a novel device capable of maintaining stable linear concentration gradients for the study of cell behavior in a 3-dimensional environment. Our work presents a significant advance over previously reported techniques because our device does not require continuous fluid flow and allows stable concentration gradients to be formed in a 3-dimensional environment for a period of days (Li Jeon et al. 2002; Mao et al. 2003; Lin et al. 2004; Zhu et al. 2004; Biddiss and Li 2005; Chung et al. 2005; Diao et al. 2006; Irimia et al. 2006; Lin and Butcher 2006; Saadi et al. 2006; Amarie et al. 2007; Cheng et al. 2007; Chung et al. 2007; Herzmark et al. 2007; Li et al. 2007, 2008; Park et al. 2007; Yang et al. 2007; Cheng et al. 2008; Fok et al. 2008; Kang et al. 2008; Liu et al. 2008; Motoo et al.

2008; Shamloo et al. 2008; Sun et al. 2008; Atencia et al. 2009; Cooksey et al. 2009; Englert et al. 2009; Glawdel et al. 2009; Haessler et al. 2009; Hattori et al. 2009; Jeon et al. 2009; Joong Yull et al. 2009; Kalinin et al. 2009; Kim et al. 2009a; Park et al. 2009; Siyan et al. 2009; Yusuf et al. 2009; Zhou et al. 2009). Other devices produce gradients without continuous flow but are still limited to 2-dimensional geometries (with limited degrees of gradient stability) (Abhyankar et al. 2006; Frevert et al. 2006; Wu et al. 2006; Du et al. 2009; Kim et al. 2009b), while others establish gradients in 3-dimensional environments but are dependent on fluid flow (Mosadegh et al. 2007; Saadi et al. 2007; Tingjiao et al. 2009; He et al. 2010; Zervantonakis et al. 2010). The incorporation of low resistance reservoir paths prevents convective transport of soluble factors through the hydrogel region and the disruption of the concentration profile by pressure gradients. This result is achieved without the incorporation of multilayered microfluidic chips, specialized pressure regulators, valves, or continuous fluid flow. The simple design coupled with the device's resistance to perturbations during handling make the RC device optimal for cell biology applications, with no prerequisite expertise in microfluidic technology required. Here we have performed chemotaxis assays with three different cell types, which each behave differently in culture. Vascular smooth muscle cells attach to flat substrates and grow in a 2-dimensional monolayer whereas endothelial cells have the ability to form a monolayer on 3-dimensional surfaces (Chung et al. 2009). Jurkat T lymphocytes that are normally cultured in suspension were also able to adhere to and invade the collagen gel. In addition to these and other cell types, the versatility of the RC device also lends itself to the study of explant biology and other 3-dimensional cellular aggregates such as embryoid bodies. To demonstrate this we differentiated embryonic stem cells as 3-dimensional aggregates in the gel region and superimposed a Shh morphogen gradient to show, for the first time, differential expression of neural tube transcription factors in a Shh concentration gradient in 3-dimensional differentiation cultures. Our results confirm the accepted paradigm governing the role of Shh in neural development and future studies with more complex gradients will help elucidate the role of additional signaling gradients, such as fibroblast growth factors, bone morphogenic proteins, and Wnts, that affect the spatiotemporal patterning in the neural tube (Joong Yull et al. 2009; Ulloa and MartÌ 2010).

Finally the device design is amenable to simple modifications to enhance its performance for specific applications. While we have explored migratory events occurring over 1 day to 2 days and differentiation occurring over the course of 3 days to 4 days, some processes might require longer observation periods. By increasing the sizes of the source and sink wells relative to that of the gel region a steep gradient can be maintained for longer periods of time as the flux of solute now occurs between two larger volumes. Additionally, the integration of larger wells increases the availability of media and nutrients, slows the accumulation of waste products, and eliminates the need for frequent media changes. Although increasing the well volumes would also reduce pressure gradients caused by volume imbalances, this would not eliminate the need for the low resistance bypass channels unless the wells were increased dramatically. Using Darcy's Law the Peclet number, *Pe*, for mass transport through the gel can be written as a function of a volume imbalance ΔV and the diameter of the wells,

$$Pe=\frac{4K\rho g\Delta V}{D\pi D_w^2\mu}.$$

For convection and diffusion to balance (*Pe*=1) in the presence of a 10 μl bolus and for a molecule with a diffusivity of 1.6×10^{-6} cm^2/s, the diameter of the wells would need to be 2.8 cm which is nearly ten times the size of the wells in this paper.

To create alternative concentration profiles such as intersecting or exponential gradients the geometry and number of gel regions can be changed as we have demonstrated. Together, the simplicity of the design that eliminates solute convection through the gel, the variety of biological systems that can be incorporated into the device, and the adaptability of the device to new designs that can modulate gradient formation create an effective tool for interrogating the behavior of cells within a defined 3D microenvironment and under the influence of a stable concentration gradient.

Supplementary Material

Refer to Web version on PubMed Central for supplementary material.

Acknowledgments

This work was supported by National Institute of Health Grants EB003805, AG032977, T32EB006348, R01 AG032977, R37 NS054364, and F31HL095342.

References

Abbott A. Cell culture: biology's new dimension. Nature. 2003; 424(6951):870–872. [PubMed: 12931155]

Abhyankar VV, Lokuta MA, et al. Characterization of a membrane-based gradient generator for use in cell-signaling studies. Lab Chip. 2006; 6(3):389–393. [PubMed: 16511622]

Abhyankar VV, Toepke MW, et al. A platform for assessing chemotactic migration within a spatiotemporally defined 3D microenvironment. Lab Chip. 2008; 8(9):1507–1515. [PubMed: 18818806]

Amarie D, Glazier JA, et al. Compact microfluidic structures for generating spatial and temporal gradients. Anal Chem. 2007; 79(24):9471–9477. [PubMed: 17999467]

Atencia J, Morrow J, et al. The microfluidic palette: a diffusive gradient generator with spatiotemporal control. Lab Chip. 2009; 9(18):2707–2714. [PubMed: 19704987]

Biddiss E, Li D. Electrokinetic generation of temporally and spatially stable concentration gradients in microchannels. J Colloid Interface Sci. 2005; 288(2):606–615. [PubMed: 15927632]

Bornfeldt KE, Raines EW, Nakano T, Graves LM, Krebs EG, Ross R. Insulin-like growth factor-I and platelet-derived growth factor-BB induce directed migration of human arterial smooth muscle cells via signaling pathways that are distinct from those of proliferation. J Clin Invest. 1994; 93(3):1266–1274. [PubMed: 8132765]

Boyden S. The chemotactic effect of mixtures of antibody and antigen on polymorphonuclear leucocytes. J Exp Med. 1962; 113(3):453–466. [PubMed: 13872176]

Briscoe J. Making a grade: Sonic Hedgehog signalling and the control of neural cell fate. EMBO J. 2009; 28(5):457–465. [PubMed: 19197245]

Cheng SY, Heilman S, et al. A hydrogel-based microfluidic device for the studies of directed cell migration. Lab Chip. 2007; 7(6):763–769. [PubMed: 17538719]

Cheng JY, Yen MH, et al. A transparent cell-culture microchamber with a variably controlled concentration gradient generator and flow field rectifier. Biomicrofluidics. 2008; 2(2):24105. [PubMed: 19693408]

Chung BG, Flanagan LA, et al. Human neural stem cell growth and differentiation in a gradient-generating microfluidic device. Lab Chip. 2005; 5(4):401–406. [PubMed: 15791337]

Chung BG, Manbachi A, et al. A gradient-generating microfluidic device for cell biology. J Vis Exp. 2007; 7:271. [PubMed: 18989442]

Chung S, Sudo R, et al. Cell migration into scaffolds under co-culture conditions in a microfluidic platform. Lab Chip. 2009; 9(2):269–275. [PubMed: 19107284]

Cooksey GA, Sip CG, et al. A multi-purpose microfluidic perfusion system with combinatorial choice of inputs, mixtures, gradient patterns, and flow rates. Lab Chip. 2009; 9(3):417–426. [PubMed: 19156291]

Cukierman E, Pankov R, et al. Taking cell-matrix adhesions to the third dimension. Science. 2001; 294(5547):1708–1712. [PubMed: 11721053]

Dessaud E, Yang LL, et al. Interpretation of the sonic hedgehog morphogen gradient by a temporal adaptation mechanism. Nature. 2007; 450(7170):717–720. [PubMed: 18046410]

Dessaud E, McMahon AP, et al. Pattern formation in the vertebrate neural tube: a sonic hedgehog morphogen-regulated transcriptional network. Development. 2008; 135(15):2489–2503. [PubMed: 18621990]

Diao J, Young L, et al. A three-channel microfluidic device for generating static linear gradients and its application to the quantitative analysis of bacterial chemotaxis. Lab Chip. 2006; 6(3):381–388. [PubMed: 16511621]

Du Y, Shim J, et al. Rapid generation of spatially and temporally controllable long-range concentration gradients in a microfluidic device. Lab Chip. 2009; 9(6):761–767. [PubMed: 19255657]

Englert DL, Manson MD, et al. Flow-based microfluidic device for quantifying bacterial chemotaxis in stable, competing gradients. Appl Environ Microbiol. 2009; 75(13):4557–4564. [PubMed: 19411425]

Even-Ram S, Yamada KM. Cell migration in 3D matrix. Curr Opin Cell Biol. 2005; 17(5):524–532. [PubMed: 16112853]

Fok S, Domachuk P, et al. Planar microfluidic chamber for generation of stable and steep chemoattractant gradients. Biophys J. 2008; 95(3):1523–1530. [PubMed: 18645198]

Frevert CW, Boggy G, et al. Measurement of cell migration in response to an evolving radial chemokine gradient triggered by a microvalve. Lab Chip. 2006; 6(7):849–856. [PubMed: 16804588]

Friedl P, Weigelin B. Interstitial leukocyte migration and immune function. Nat Immunol. 2008; 9(9): 960–969. [PubMed: 18711433]

Gabriel GM, John K. Endothelial cell protrusion and migration in three-dimensional collagen matrices. Cell Motil Cytoskeleton. 2006; 63(2):101–115. [PubMed: 16395720]

Garanich JS, Pahakis M, et al. Shear stress inhibits smooth muscle cell migration via nitric oxide-mediated downregulation of matrix metalloproteinase-2 activity. Am J Physiol Heart Circ Physiol. 2005; 288(5):H2244–2252. [PubMed: 15637127]

Ghibaudo M, Trichet L, et al. Substrate topography induces a crossover from 2D to 3D behavior in fibroblast migration. Biophys J. 2009; 97(1):357–368. [PubMed: 19580774]

Glawdel T, Elbuken C, et al. Microfluidic system with integrated electroosmotic pumps, concentration gradient generator and fish cell line (RTgill-W1)-towards water toxicity testing. Lab Chip. 2009; 9(22):3243–3250. [PubMed: 19865731]

Haessler U, Kalinin Y, et al. An agarose-based microfluidic platform with a gradient buffer for 3D chemotaxis studies. Biomed Microdevices. 2009; 11(4):827–835. [PubMed: 19343497]

Hai-Qing X, Elizabeth M, et al. A Subset of ES-Cell-derived neural cells marked by gene targeting. Stem Cells. 2003; 21(1):41–49. [PubMed: 12529550]

Hattori K, Sugiura S, et al. Generation of arbitrary monotonic concentration profiles by a serial dilution microfluidic network composed of microchannels with a high fluidic-resistance ratio. Lab Chip. 2009; 9(12):1763–1772. [PubMed: 19495461]

He J, Du Y, et al. Rapid generation of biologically relevant hydrogels containing long-range chemical gradients. Adv Funct Mater. 2010; 20(1):131–137. [PubMed: 20216924]

Herzmark P, Campbell K, et al. Bound attractant at the leading vs. the trailing edge determines chemotactic prowess. PNAS. 2007; 104(33):13349–54. [PubMed: 17684096]

Hesselgesser J, Liang M, et al. Identification and characterization of the CXCR4 chemokine receptor in human T cell lines: ligand binding, biological activity, and HIV-1 infectivity. J Immunol. 1998; 160(2):877–883. [PubMed: 9551924]

Irimia D, Geba DA, et al. Universal microfluidic gradient generator. Anal Chem. 2006; 78(10):3472–3477. [PubMed: 16689552]

Jeon H, Lee Y, et al. Quantitative analysis of single bacterial chemotaxis using a linear concentration gradient microchannel. Biomed Microdevices. 2009; 11(5):1135–1143.

Joong Yull P, Suel-Kee K, et al. Differentiation of neural progenitor cells in a microfluidic chip-generated cytokine gradient. Stem Cells. 2009; 27(11):2646–2654. [PubMed: 19711444]

Kalinin YV, Jiang L, et al. Logarithmic sensing in escherichia coli bacterial chemotaxis. Biophys J. 2009; 96(6):2439–2448. [PubMed: 19289068]

Kang T, Han J, et al. Concentration gradient generator using a convective-diffusive balance. Lab Chip. 2008; 8(7):1220–1222. [PubMed: 18584102]

Keenan TM, Folch A. Biomolecular gradients in cell culture systems. Lab Chip. 2008; 8(1):34–57. [PubMed: 18094760]

Kim D, Lokuta MA, et al. Selective and tunable gradient device for cell culture and chemotaxis study. Lab Chip. 2009a; 9(12):1797–1800. [PubMed: 19495465]

Kim T, Pinelis M, et al. Generating steep, shear-free gradients of small molecules for cell culture. Biomed Microdevices. 2009b; 11(1):65–73. [PubMed: 18688724]

Laird DJ, von Andrian UH, et al. Stem cell trafficking in tissue development, growth, and disease. Cell. 2008; 132(4):612–630. [PubMed: 18295579]

Lee J, Cuddihy MJ, et al. Three-dimensional cell culture matrices: state of the art. Tissue Eng B Rev. 2008; 14(1):61–86.

Li Jeon N, Baskaran H, et al. Neutrophil chemotaxis in linear and complex gradients of interleukin-8 formed in a microfabricated device. Nat Biotech. 2002; 20(8):826–830.

Li CW, Chen R, et al. Generation of linear and non-linear concentration gradients along microfluidic channel by micro-tunnel controlled stepwise addition of sample solution. Lab Chip. 2007; 7(10): 1371–1373. [PubMed: 17896024]

Li G, Liu J, et al. Multi-molecular gradients of permissive and inhibitory cues direct neurite outgrowth. Ann Biomed Eng. 2008; 36(6):889–904. [PubMed: 18392680]

Lin F, Butcher EC. T-cell chemotaxis in a simple microfluidic device. Lab Chip. 2006; 6(11):1462–1469. [PubMed: 17066171]

Lin F, Saadi W, et al. Generation of dynamic temporal and spatial concentration gradients using microfluidic devices. Lab Chip. 2004; 4(3):164–167. [PubMed: 15159771]

Liu Y, Sai J, et al. Microfluidic switching system for analyzing chemotaxis responses of wortmannin-inhibited HL-60 cells. Biomed Microdevices. 2008; 10(4):499–507. [PubMed: 18205049]

Mack PJ, Zhang Y, et al. Biomechanical regulation of endothelium-dependent events critical for adaptive remodeling. J Biol Chem. 2009; 284(13):8412–8420. [PubMed: 19047056]

Mao H, Cremer PS, et al. A sensitive, versatile microfluidic assay for bacterial chemotaxis. Proc Natl Acad Sci USA. 2003; 100(9):5449–5454. [PubMed: 12704234]

Montero JA, Heisenberg CP. Gastrulation dynamics: cells move into focus. Trends Cell Biol. 2004; 14(11):620–627. [PubMed: 15519851]

Mosadegh B, Huang C, et al. Generation of stable complex gradients across two-dimensional surfaces and three-dimensional gels. Langmuir. 2007; 23(22):10910–10912. [PubMed: 17910490]

Motoo K, Toda N, et al. Generation of concentration gradient from a wave-like pattern by high frequency vibration of liquid–liquid interface. Biomed Microdevices. 2008; 10(3):329–335. [PubMed: 18071908]

Nelson RD, Quie PG, et al. Chemotaxis under agarose: a new and simple method for measuring chemotaxis and spontaneous migration of human polymorphonuclear leukocytes and monocytes. J Immunol. 1975; 115(6):1650–1656. [PubMed: 1102606]

O'Hayre M, Salanga CL, et al. Chemokines and cancer: migration, intracellular signalling and intercellular communication in the microenvironment. Biochem J. 2008; 409(3):635–649. [PubMed: 18177271]

Park JY, Hwang CM, et al. Gradient generation by an osmotic pump and the behavior of human mesenchymal stem cells under the fetal bovine serum concentration gradient. Lab Chip. 2007; 7(12):1673–1680. [PubMed: 18030386]

Park JY, Yoo SJ, et al. Simultaneous generation of chemical concentration and mechanical shear stress gradients using microfluidic osmotic flow comparable to interstitial flow. Lab Chip. 2009; 9(15): 2194–2202. [PubMed: 19606296]

Saadi W, Wang SJ, et al. A parallel-gradient microfluidic chamber for quantitative analysis of breast cancer cell chemotaxis. Biomed Microdevices. 2006; 8(2):109–118. [PubMed: 16688570]

Saadi W, Rhee S, et al. Generation of stable concentration gradients in 2D and 3D environments using a microfluidic ladder chamber. Biomed Microdevices. 2007; 9(5):627–635. [PubMed: 17530414]

Shamloo A, Ma N, et al. Endothelial cell polarization and chemotaxis in a microfluidic device. Lab Chip. 2008; 8(8):1292–1299. [PubMed: 18651071]

Siyan W, Feng Y, et al. Application of microfluidic gradient chip in the analysis of lung cancer chemotherapy resistance. J Pharm Biomed Anal. 2009; 49(3):806–810. [PubMed: 19162424]

Smalley KSM, Lioni M, et al. Life isn't flat: taking cancer biology to the next dimension. *In Vitro* Cell. Dev Biol Anim. 2006; 42(8):242–247.

Sudo R, Chung S, et al. Transport-mediated angiogenesis in 3D epithelial coculture. FASEB J. 2009; 23(7):2155–2164. [PubMed: 19246488]

Sun S, Wise J, et al. Human fibroblast migration in three-dimensional collagen gel in response to noninvasive electrical stimulus. I. Characterization of induced three-dimensional cell movement. Tissue Eng. 2004; 10(9–10):1548–1557. [PubMed: 15588414]

Sun K, Wang Z, et al. Modular microfluidics for gradient generation. Lab Chip. 2008; 8(9):1536–1543. [PubMed: 18818810]

Tingjiao L, Chunyu L, et al. A microfluidic device for characterizing the invasion of cancer cells in 3-D matrix. Electrophoresis. 2009; 30(24):4285–4291. [PubMed: 20013914]

Ulloa F, MartÌ E. Wnt won the war: antagonistic role of Wnt over Shh controls dorso-ventral patterning of the vertebrate neural tube. Dev Dyn. 2010; 239(1):69–76. [PubMed: 19681160]

Veldkamp CT, Seibert C, et al. Structural basis of CXCR4 sulfotyrosine recognition by the chemokine SDF-1/CXCL12. Sci Signal. 2008; 1(37):ra4. [PubMed: 18799424]

Vernon RB, Sage EH. A novel quantitative model for study of endothelial cell migration and sprout formation within three-dimensional collagen matrices. Microvasc Res. 1999; 57(2):118–133. [PubMed: 10049660]

Vickerman V, Blundo J, et al. Design, fabrication and implementation of a novel multi-parameter control microfluidic platform for three-dimensional cell culture and real-time imaging. Lab Chip. 2008; 8(9):1468–1477. [PubMed: 18818801]

Vokes SA, Ji H, et al. Genomic characterization of Gli-activator targets in sonic hedgehog-mediated neural patterning. Development. 2007; 134:1977–1989. [PubMed: 17442700]

Wang S, Tarbell JM. Effect of fluid flow on smooth muscle cells in a 3-dimensional collagen gel model. Arterioscler Thromb Vasc Biol. 2000; 20(10):2220–2225. [PubMed: 11031207]

Wu H, Huang B, et al. Generation of complex, static solution gradients in microfluidic channels. J Am Chem Soc. 2006; 128(13):4194–4195. [PubMed: 16568971]

Yang J, Pi X, et al. Diffusion characteristics of a T-type microchannel with different configurations and inlet angles. Anal Sci. 2007; 23(6):697–703. [PubMed: 17575354]

Yusuf HA, Baldock SJ, et al. Optimisation and analysis of microreactor designs for microfluidic gradient generation using a purpose built optical detection system for entire chip imaging. Lab Chip. 2009; 9(13):1882–1889. [PubMed: 19532963]

Zaman MH, Kamm RD, et al. Computational model for cell migration in three-dimensional matrices. Biophys J. 2005; 89(2):1389–1397. [PubMed: 15908579]

Zaman MH, Trapani LM, et al. Migration of tumor cells in 3D matrices is governed by matrix stiffness along with cell-matrix adhesion and proteolysis. Proc Natl Acad Sci. 2006; 103(29):10889–10894. [PubMed: 16832052]

Zervantonakis I, Chung S, et al. Concentration gradients in microfluidic 3D matrix cell culture systems. Intern J Micro-Nano Scale Transport. 2010; 1(1):27–36.

Zhang, S.; George, FVW., et al. Adv Cancer Res. Vol. 99. Academic Press; 2008. Designer Self-assembling peptide nanofiber scaffolds for study of 3-D cell biology and beyond; p. 335-362.

Zhou Y, Wang Y, et al. Generation of complex concentration profiles by partial diffusive mixing in multi-stream laminar flow. Lab Chip. 2009; 9(10):1439–1448. [PubMed: 19417912]

Zhu X, Chu LY, et al. Arrays of horizontally-oriented mini-reservoirs generate steady microfluidic flows for continuous perfusion cell culture and gradient generation. Analyst. 2004; 129(11):1026–1031. [PubMed: 15508030]

Zicha D, Dunn GA, et al. A new direct-viewing chemotaxis chamber. J Cell Sci. 1991; 99(4):769–775. [PubMed: 1770004]

Zigmond SH. Ability of polymorphonuclear leukocytes to orient in gradients of chemotactic factors. J Cell Biol. 1977; 75(2):606–616. [PubMed: 264125]

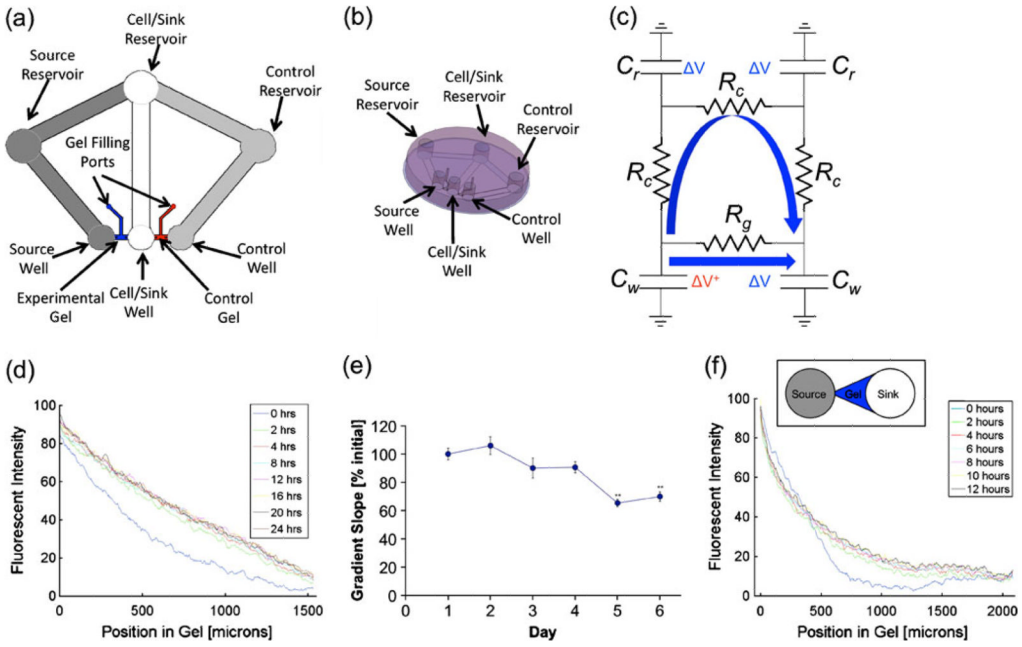

Fig. 1.

RC Device design and stable gradient formation. (**a**) A schematic representation of the RC device layout in 2D. The *unshaded* channels represent the sink and sink reservoir connected by the sink channel. The *dark shaded* region represents the source and source reservoir/ channel as well as a channel connecting the source and sink reservoirs. The *lightly shaded* region is the mirror image of the dark shaded source region and serves as an internal control for each experiment. The *blue region* is the location of the hydrogel in which the relevant concentration gradient forms, and the *red region* is the analogous control hydrogel. The chemical species of interest is placed in the source well and source reservoir. The remainder of the device is filled with a control solution. During cell migration experiments, cells are loaded into the cell/sink well and after an incubation period the distribution of cells in the experimental and control gels is analyzed. (**b**) A 3D representation of the RC device constructed from PDMS and bonded to a glass coverslip. The diameter of the source, sink, and control wells is 3 mm, and the diameter of the source, sink, and control reservoirs is 4 mm. The hydrogel channels are 1.5 mm long, 0.6 mm wide, and 0.120 mm tall. The remaining channels are 20 mm long, 2 mm wide, and 0.120 mm tall. (**c**) An analogous RC electrical circuit can be used to depict how the low resistance channels dissipate pressure gradients more rapidly than the high resistance gel region. (**d**) A 10 kDa FITC-dextran molecule was used to model the diffusion of a similarly sized protein such as SDF-1. The dextran solution (25 μg/ml) was loaded into the source well and source reservoir. The sink well, control well, sink reservoir, and control reservoir were filled with PBS. The device was placed on a fluorescent microscope and images were acquired every hour (representative time points shown) for 24 h. To prevent evaporation the device was covered with a glass cover slip during image acquisition. Within 2 h a linear concentration profile is achieved in the gel region and maintained for the duration of the experiment. (**e**) The dextran gradient was tracked over the course of 6 days and the average slope of the concentration profile is shown for each day. The slope remains constant for the first 48 h and on day 3 the slope has decayed by 10%. **P<0.01 (**f**) By changing the geometry of the gel region (as shown in the inset) a non-linear concentration profile with an exponential dependency was achieved in the RC device. Fluorescent images were acquired every 2 h for 12 h

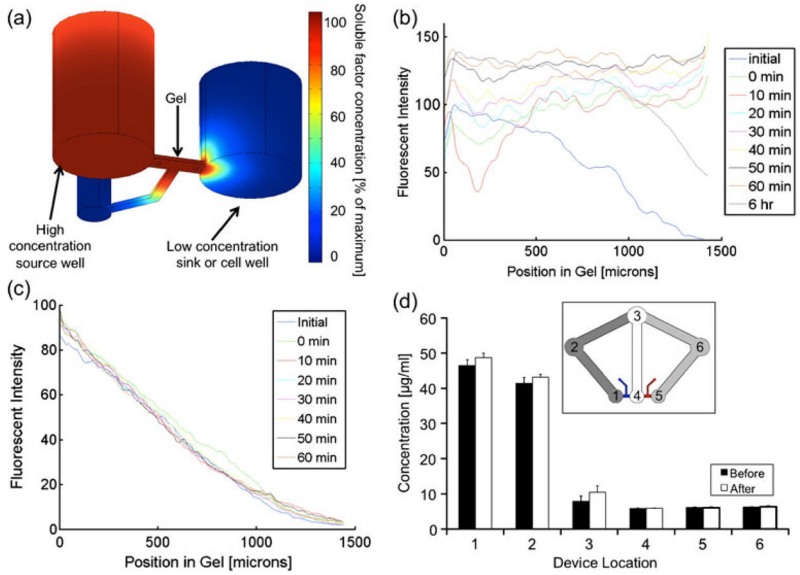

Fig. 2.

Dissipation of pressure gradients in RC device without the low resistance bypass channels. (**a**) Initially the gel region and the sink well did not contain any solute. The high concentration source well was loaded with a 1 mm hydrostatic pressure difference relative to the sink well. Without the low resistance circuit the pressure difference must be dissipated via fluid flow through gel region. This fluid flow is accompanied by convection of the solute into the gel. The solute is modeled as SDF-1 with a diffusivity of 1.6×10^{-6} cm^2/s and the permeability of the gel region is 1×10^{-12} m^2. The simulation was executed for 1 h. (**b**) A gradient was allowed to develop across the experimental gel region for 6 h by placing a 25 µg/ml FITC-dextran solution in the source well of a device *without* the bypass channels. Then 10 µl of the dextran solution was added to the source well and the gradient was imaged every 10 min for an additional hour. The gradient is disrupted and after 6 h does not return to its original profile. (**c**) In the RC device with the bypass channels although the concentration profile changed slightly, within 10 min the gradient returned to a linear profile after the introduction of a 10 µl bolus. Images were acquired every 10 min for 1 h after the introduction of the bolus (**d**) The source well and reservoir were filled with a 50 µg/ml solution of FITC-dextran and the concentrations in all of the wells and reservoirs were measured before and after the addition of a 10 µl injection into the source well. The sink reservoir (location 3) experiences the greatest concentration change while the concentrations in the sink well, control well, and control reservoir remain relatively unchanged

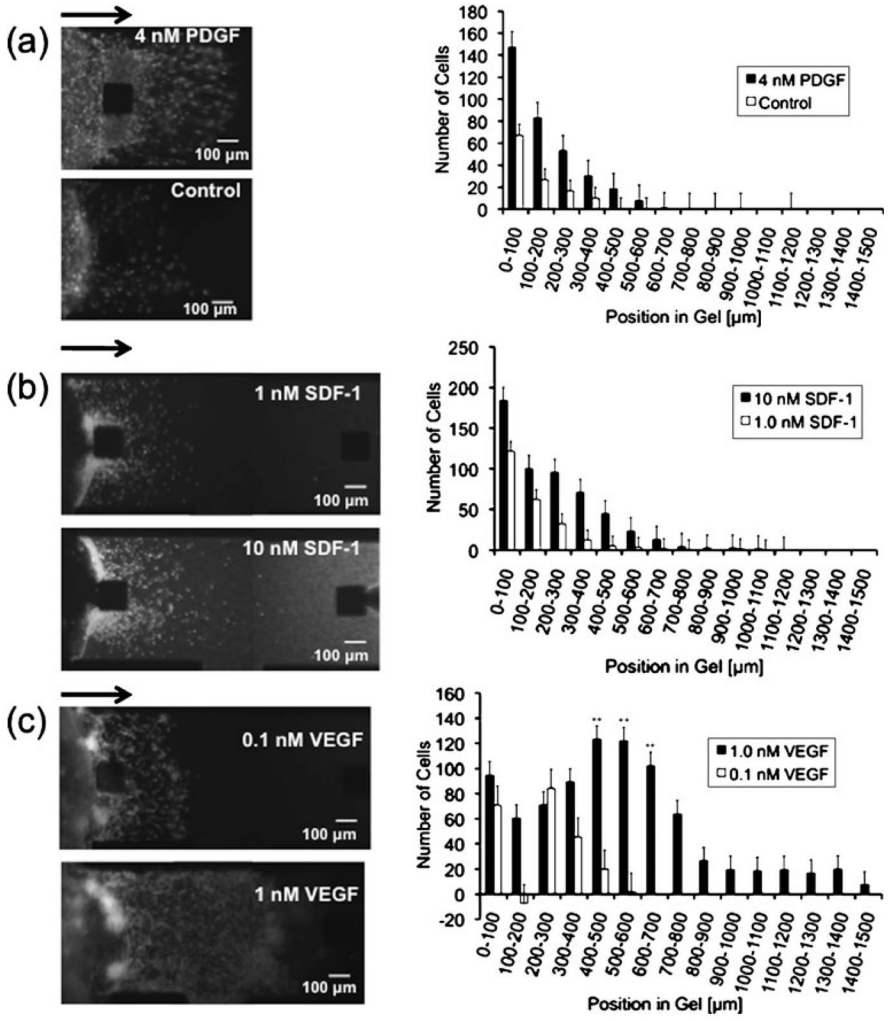

Fig. 3.

The RC Device demonstrates migration of three different cell types: vascular smooth muscle cells, Jurkat T-lymphocytes, and bovine aortic endothelial cells. (**a**) Vascular smooth muscle cells were loaded into the sink well of the RC Device and media supplemented with 4 nM of PDGF-BB was added to the source well and reservoir. The sink and control wells and reservoirs were filled with control media. (*Left*) Migration of vascular smooth muscle cells from left to right toward 4 nM PDGF-BB and the matching control from a sample device. (*Right*) Comparison of migration toward PDGF-BB vs control. The number of cells at each location decreases with increasing distance into the gel. A particularly marked difference between the PDGF and control gels is observed in the first 200 µm of the gel region. n=4. (**b**) (**a**) *Left*. Migration of Jurkat T lymphocytes from left to right toward a 1 nM solution of SDF-1 and a 10 nM solution of SDF-1. *Right*. Dose response of Jurkat T lymphocyte migration toward SDF-1 concentrations. (**c**) *Left*. Migration of bovine aortic endothelial cells from left to right toward a 0.1 nM solution of VEGF and a 1 nM solution of VEGF. *Right*. Dose response of migration of bovine aortic endothelial cells toward VEGF concentrations. 10X. White = DAPI. **P<0.01, arrows indicate direction of migration

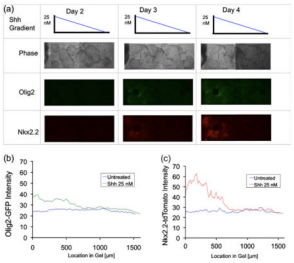

Fig. 4.

Sonic hedgehog gradients in the RC device produce graded expression of neural transcription factors. (**a**) ES cell reporter lines (Olig2-GFP and Nkx2.2-tdTomato) were mixed and differentiated in hanging drops. Two days later (day 0 of Shh exposure), embryoid bodies we seeded in collagen gels and exposed to a concentration gradient ranging from 25 nM to 0 nM along the length of the gel. On day 3, Olig2 and Nkx2.2 expression were evident by fluorescent signal at the higher concentration region in the gel. On day 4 this expression had increased in intensity and penetration into the gel as regions of lower Shh concentration received sufficient temporal exposure to induce a response. Measured day 4 expression for Olig2 (**b**) and Nkx2.2 (**c**) compared to untreated gels shows the extent of differentiation at different points in the gradient by plotting reporter fluorescent intensity vs. distance from the Shh source. Expression is highest at the locations in the gel closest to the Shh source and eventually falls to the baseline level present in the gels that contained embryoid bodies that were not simulated with Shh. This indicates the location in the gel where the Shh concentration is equal to the threshold level necessary to induce Olig2 and Nkx2.2 expression

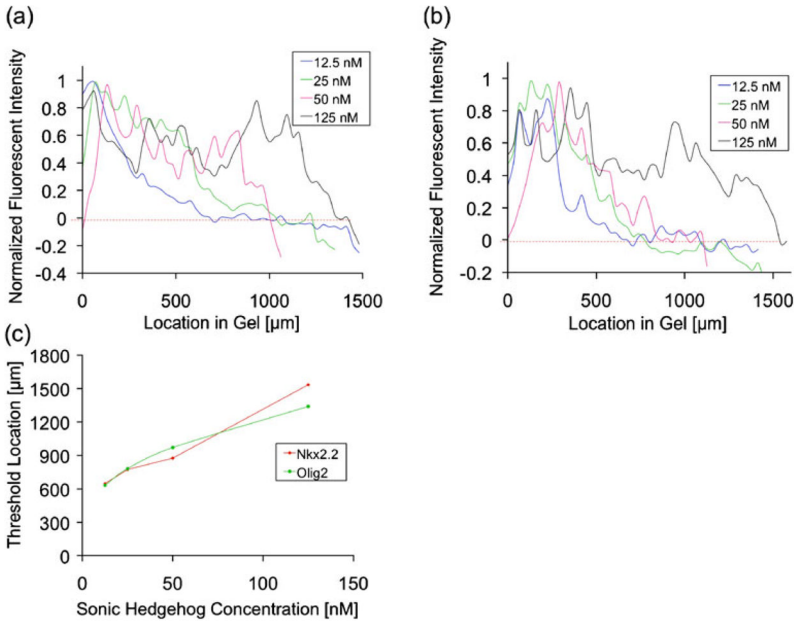

Fig. 5.

Gradients formed by different concentrations of Sonic hedgehog produced a dose response in the expression of neural transcription factors. Two day old embryioid bodies were seeded in the gel regions of the RC device and exposed to Shh gradients produced by 12.5 nM (*blue*), 25 nM (*green*), 50 nM (*pink*), and 125 nM (*black*) Shh concentrations in the source well. After 4 days of Shh exposure Olig2 (**a**) and Nkx2.2 (**b**) expression in the gel region as judged by fluorescent reporter intensity was plotted against distance from the source well. The expression levels at all four of the Shh doses were highest in the in the regions adjacent to the source wells and decreased to the baseline levels present in the gels with untreated embryoid bodies (*red dashed line*). Increasing Shh doses increased the Shh concentration at each location in the gel. Thus at higher concentrations the location of the expression threshold moves farther form the source well and the Olig2 and Nkx2.2 expression extends farther into the gel. (**c**) The location of the threshold concentration as a function of the Shh source concentration exhibits a linear relationship for both Olig2 and Nkx2.2 confirming a constant threshold concentration of approximately 10 nM Shh